

The influence of scale and the spatial characteristics of landscapes on land-cover mapping using remote sensing

Aaron Moody¹ and Curtis E. Woodcock²

¹*Department of Geography, University of North Carolina at Chapel Hill, NC 27599-3220, USA;*

²*Department of Geography and Center for Remote Sensing, Boston University, 02215, USA*

Keywords: scale, spatial pattern, proportion error, regression tree, indicator variable, remote sensing, land-cover

Abstract

Statistical analyses provide a means for assessing relationships between landscape spatial pattern and errors in the estimates of cover-type proportions as land-cover data are aggregated to coarser scales. Results from a multiple-linear regression model suggest that as patch sizes, variance/mean ratio, and initial proportions of cover types increase, the proportion error moves in a positive direction and is governed by the interaction of the spatial characteristics and the scale of aggregation. However, the standard linear model does not account for the different directions of scale-dependent proportion error since some classes become larger and others become smaller as the scene is aggregated. Addition of indicator variables representing class-type significantly improves the performance by allowing the model to respond differently to different classes. A regression tree model provides a much simpler fit to the complex scaling behavior through an interaction between patch size and aggregation scale. An understanding of the relationships between landscape pattern, scale, and proportion error may advance methods for correcting land-cover area estimates. Such methods could also facilitate high-resolution calibration and validation of coarse-scale remote-sensing-based land-cover mapping algorithms. Ongoing initiatives to produce global land-cover datasets from remote sensing, such as efforts within the IGBP and the EOS MODIS Land-Team, include significant emphasis on high level calibration and validation activities of this nature.

Introduction

In landscape studies, the representation of land-surface properties and ecological processes is linked inherently to the scale of analysis (Meentemeyer and Box 1987; Milne 1992). These scale dependencies indicate a need to incorporate scaling effects in landscape research (Turner *et al.* 1989a; Turner *et al.* 1991; Cullinan and Thomas 1992). This issue is especially relevant as increasing emphasis is placed on investigating regional to global-scale land-surface processes and patterns using remote sensing. In particular, the validation and evaluation of

global land-cover maps derived from satellite imagery must incorporate an understanding of the relationships between the scale of observation, the spatial organization of land-cover classes, and classification error. For example, in the validation of global land-cover datasets, high resolution reference data must be used to evaluate the performance of classification algorithms which operate at coarse scales. This type of validation requires methods for aggregating reference maps from fine to coarse scales, as well as knowledge of the types and magnitudes of errors that this scaling will introduce into the reference data. Similarly, an under-

standing of how the inference of landscape patterns and properties varies as a function of observation scale is necessary to characterize the accuracy and potential errors in global land-cover datasets.

Previous work (Moody and Woodcock 1994) shows that large proportion errors can arise as landscapes are represented at increasingly coarse scales. Additionally, the direction and magnitude of these errors appear to vary as a function of both the spatial pattern of the land-cover classes and the spatial resolution. This paper more formally explores the relationships between proportion error, landscape pattern, and observation scale. The intent is to understand the causes of these errors as part of a broader goal of preserving land-cover information across observation scales. The study site is the Plumas National Forest, located in a forested landscape in the Sierra Nevada Mountains in California. Measures of spatial pattern include the actual class proportions, patch size, interpatch distance, variance/mean ratio, and the Shannon index. We examine these spatial properties in terms of their influence on the scale-dependence of cover-type proportion estimates, and investigate the utility of multiple-linear regression and regression tree techniques for modeling these relationships. It is hoped that this work will lead to an improved understanding of how the spatial organization of landscapes influences the nature and magnitude of proportion errors in maps derived from remote sensing. Our particular interest is the effect of these scaling characteristics on the representation of landscapes at regional to global scales.

Landscape scaling issues take on special importance as efforts are advanced to develop improved representations of global land-cover. Global monitoring activities, such as those of the IGBP (International Geosphere-Biosphere Program) and the Land Group of the MODIS Science Team (Moderate Resolution Imaging Spectroradiometer) will require a knowledge of the error content of land-cover datasets produced by these groups (Townshend 1992; Strahler *et al.* 1994; Running *et al.* 1994). MODIS is scheduled for launch on board the EOS-AM (Earth Observing System) platform in 1998 and will be the primary EOS instrument for monitoring terrestrial activity at the global scale.

Methods for producing global land-cover datasets using MODIS measurements are currently under development and local-scale calibration and validation are key components of algorithm design and product evaluation (Strahler *et al.* 1994). Calibration and validation activities will require comparisons of land-cover maps across spatial scales and an understanding of the effect of scaling thematic land-cover data is considered important for their success. It is in the context of these issues that we present this research.

While remote sensing is well suited for characterizing landscapes at broad scales, our understanding of the interaction between the spatial resolution of satellite sensors and landscape pattern is limited. This interaction is governed by a convolution of scene-independent processes, such as atmospheric effects and sensor response characteristics, and scene-dependent processes, such as the spectral and spatial mixing of sub-pixel scene components. In this research, we are primarily concerned with map error as it is driven by the relationship between the spatial properties of the component cover types and the resolution of the map, or pixel size.

Background

Related work indicates that changes in proportion estimates with the aggregation of land-cover maps are related to the scale of aggregation, the initial proportions of the component types, and the spatial organization of the landscape (Turner *et al.* 1989a; Moody and Woodcock 1994). A qualitative assessment of the spatial patterns of individual land-cover types by Moody and Woodcock (1994), suggests that the influence of initial class proportion on scale-dependent proportion error is modulated by class-specific patch size, patch density and landscape diversity. These conclusions compliment findings by Turner *et al.* (1989a) who investigated the effect of changing map scales on apparent landscape pattern and class proportions for random landscapes. While the analysis of Turner *et al.* (1989a) was based on overall statistical measures for the entire scene, this paper and its precursor focus primarily on the spatial patterns of individual

land-cover classes. In reality, it is probably a combination of cover-type-specific and scene-wide (interactive) spatial patterns which control the degree of proportion error as spatial resolution becomes coarser.

A brief synopsis of the relevant literature is presented here. For a more complete review see Moody and Woodcock (1994). Various investigators have approached problems regarding the scaling of spatial data from related but distinct perspectives. In remote sensing, many researchers have investigated the influence of spatial resolution on land-cover classification accuracy. This work has been motivated in part by the need to define appropriate sampling resolutions for characterizing land surface phenomena, and also by a desire to understand and extract useful information from spatially integrated data. These efforts have involved assessing the characteristics of land-cover class maps derived from data either sampled at different resolutions by different sensors, or degraded to a series of coarser scales from a single high-resolution dataset (Latty and Hoffer 1981; Gervin *et al.* 1985; Nellis and Briggs 1989). In a somewhat different context, Marceau *et al.* (1994) investigated the impact of measurement scale and aggregation level on the information content of images and classification accuracy. Much recent work has focused on the relationship between sampling resolution and the spatial properties of scenes (Woodcock and Strahler 1987; Townshend and Justice 1988 and 1990). Scaling processes also have been investigated at a more theoretical level by several researchers including Jupp *et al.* (1988), and Raffy (1992). These works are relevant primarily to the modeling of land-surface physical processes using remotely sensed data.

In the ecological community, interest in the scaling of landscape patterns and ecological processes is driven by the expanding range of scales at which ecological analyses are conducted. Milne (1992) in a fractal analysis of landscapes, discusses the scale dependent influence of landscape pattern on ecological processes and environmental responses of organisms. These scale effects suggest first, a need to understand the complexities in combining data from multiple measurement scales, and

second, the importance of the scale dependence of landscape phenomena when investigating disturbance processes and ecosystem dynamics over large areas (Meentemeyer and Box 1987; Turner *et al.* 1989a, 1989b; Baker 1993; Field and Ehleringer 1993). Recent ecological studies which explicitly investigate these issues include work by Stoms (1994) on the scale-dependence of species richness measurements, and Baker (1993) who investigated the relationship between scale and the spatial structure of landscape response to fire suppression. In related work, Nellis and Briggs (1989) used measures of textural contrast at multiple scales to investigate different levels of landscape heterogeneity.

The research presented here is motivated primarily by a need for methods either to mitigate the loss of information due to the transference of land-surface data across scales, or to quantify the reduced information content of rescaled spatial data. Such issues are increasingly important as researchers in numerous fields attempt to compare, extrapolate and integrate data across spatial domains (Hess 1994). Our approach is to quantify the spatial characteristics of the test site using a set of simple measures, and evaluate through statistical analyses which spatial properties best explain the relationship between proportion error and spatial scale.

Methods

Site description

This research employs data from the western two-thirds of the Plumas National Forest in California (Fig. 1). The Plumas lies at the transition between the northern Sierra Nevada and the southern Cascade Range in Northern California. The transition zone represents a division between the metamorphic and granitic geology of the Sierra Nevadas and the volcanics of the Cascades. This area has high relief, drained primarily by the Feather River watershed which feeds the Sacramento System of the upper San Joaquin Valley. The vegetation can be characterized as shrub formations, pine and oak

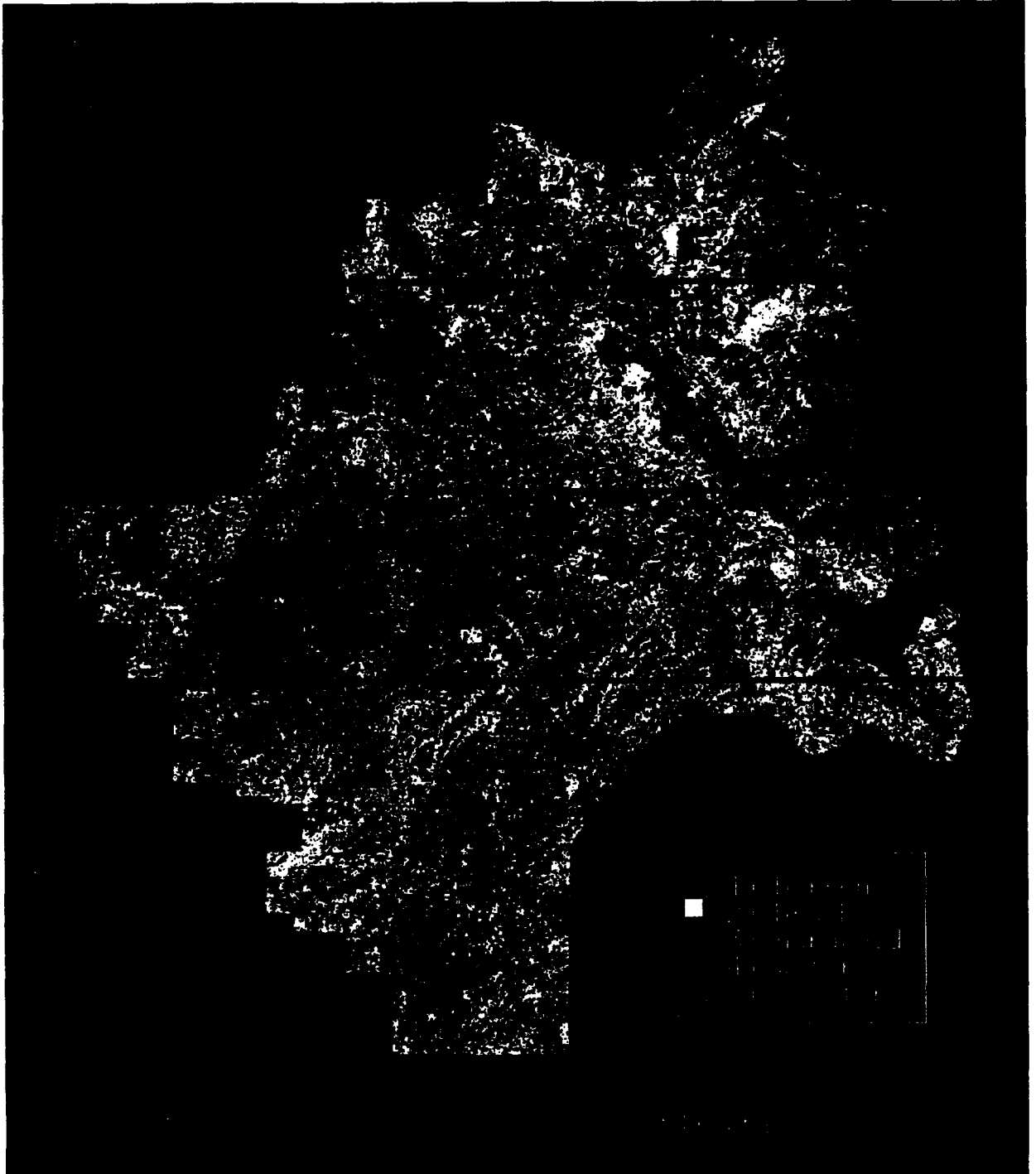


Fig. 1. Plumas National Forest study area. The symbols R1 through R4 signify the four regions of the study area.

woodlands at the lower elevations, mixed conifer and riparian hardwoods at intermediate elevations, and mixed conifer forests combined with

brush at higher elevations. Areas of brush and grasslands are distributed throughout the area, particularly at the higher elevations and in the drier

eastern region of the Forest. Barren rock outcrops exist at the highest elevations and scattered throughout the region.

The Plumas National Forest has been studied recently as part of a project to develop vegetation mapping and timber-inventory methods for the U.S. Forest Service (Woodcock *et al.* 1993). A land-cover map was produced using Landsat Thematic Mapper imagery and unsupervised image classification supported by air-photo and field validation. Cover classes include *grass/barren*, *brush*, *hardwood*, *meadow*, *conifer* and *water*. Meadows are omitted from the study due to their small size and relative infrequency. The *grass/barren* category will be referred to as *barren*. The accuracy of the Plumas National Forest map has been assessed using methods based on fuzzy sets (Gopal and Woodcock 1994). Using a stringent MAX operator, the general land-cover classes are 84% accurate (Woodcock *et al.* 1994).

Data scaling

The 30-m resolution land-cover maps were used to label a series of coarser resolution maps through a plurality-based aggregation procedure. For each new resolution of interest, a sampling grid is coded with respect to the most frequently occurring cover type among the 30-m resolution pixels within each grid cell. The resolutions considered are 90, 150, 240, 510 and 1020 meters. This allows the examination of changes in landcover proportions as a function of observation scale, or level of aggregation. The 240, 510 and 1020 m resolutions roughly coincide with the spatial resolutions of the proposed MODIS sensor (Salomonson *et al.* 1989).

Spatial measures

Changes in the estimated proportion of individual cover types with progressive aggregation are expected to depend on the typical patch size for the given class, the typical inter-patch distance, the relative randomness with which the individual classes are spatially distributed, the true proportion of the

cover types, and the diversity of the landscape (Moody and Woodcock 1994; Turner *et al.* 1989a). Simple measures used to describe these scene characteristics are defined below.

The Shannon index (H') responds to both the richness and evenness of the scene (Baker and Cai 1992; O'Neill *et al.* 1988) and is defined as:

$$H' = - \sum_{i=1}^k (P_i) \log(P_i)$$

where P_i is the fraction of the sampling area composed of class i and the total number of classes is k . The subscripts i and k are used here to maintain consistency with the rest of the notation in this paper. This measure will increase as the landscape is more evenly divided among the component cover types, and will decrease with the total number of component types, reaching zero if only one type exists.

The variance/mean ratio is a common method in point-pattern analysis to measure the degree of clustering or regularity in spatially distributed data (Unwin 1981; Getis and Boots 1978). The ratio is calculated as $vmr = s^2/\bar{m}$ where:

$$\bar{m} = \frac{\sum f_n m_n}{\sum f_n}$$

and

$$s^2 = \frac{[\sum f_n (m_n - \bar{m})^2]}{(\sum f_n - 1)}$$

where m_n is an index representing the number of class occurrences in a cell, and f_n is the number of cells with class count n . A cell size of 8×8 is used in this analysis. A vmr_i value of 1.0 indicates a random spatial pattern as the variance around the mean frequency of a given class in all cells is equal to that mean if the pattern is generated by a Poisson process. Large values of vmr_i indicate a more aggregated distribution and small values indicate a more even distribution, as the variance around the mean frequency will increase or decrease, respectively.

In the strict sense, the variance/mean ratio requires that the counts within cells are point measurements of which an infinite number are possible in each cell. In our case, counts are frequencies of

30-m pixels for each cover type within the 8×8 grid cells. This deviates from the assumptions of point-pattern analysis and undermines the use of a t test for significance of measured values of vmr_i . For this analysis we use the relative magnitudes of vmr_i and thus the deviations from the initial assumptions are not important.

Initial class proportion (P_{i0}) is simply the proportion of each cover type in the original 30-m map, and scale of aggregation (r) is the resolution of each aggregated map. Mean patch size (psz_i), mean interpatch distance ($pdst_i$), and the Shannon index (H') were all calculated using the *r.le* software developed by Baker and Cai (1992). This software was designed for the analysis of landscape data and patch dynamics and operates as an add-on to GRASS (Geographical Resource Analysis Support System) which is a public domain geographic information system (Baker and Cai 1992; USA-CERL 1991). The measures psz_i , $pdst_i$, vmr_i and P_{i0} are all class-specific measures, whereas H' is a multi-class measure.

The dependent variable is proportion estimation error (E_{ir}), defined as:

$$E_{ir} = (P_{ir} - P_{i0})/P_{i0}$$

where P_{i0} is the original proportion and P_{ir} is the estimated proportion at resolution r . While absolute proportion error, defined as $P_{i0} - P_{ir}$, represents error relative to the entire image, E_{ir} represents the proportion by which individual classes are over- or underestimated. It should be noted that the aggregation procedure may itself influence this measure and that different procedures would result in different values.

Each of the above measures is calculated for each of four subregions in the test site (Fig. 1). Considering four subregions, five cover types, and five scales (apart from the original resolution) there are a total of 100 samples used for the analysis. The dependent variable (E_{ir}) is measured for each cover type within each region at five separate scales. This provides 25 distinct measurements of the dependent variable within each region. However, the predictor variables are only measured at a single scale and therefore provide only 5 distinct measurements within each region; that is, one measurement on each pre-

dictor for each cover type within each region. The exception to this is the observation scale, r , for which there are only 5 values that do not vary between cover types or between regions. Scale (r) can be considered an ordered factor, and it is the interaction between this variable and the other predictors which drives the scaling process and is of primary interest.

Statistical models

Multiple-linear and tree-based regression techniques were used to investigate the influence of landscape spatial pattern on scale-dependent changes in the areal estimates of land-cover types. A linear model was developed using stepwise regression procedures to identify the set of independent variables which contribute significantly to the estimation of the dependent variable. This model is usually referred to as the 'standard' model below. Indicator variables representing class type were introduced into the standard model in order to test the class independence of the explanatory variables and to develop an improved model incorporating important class dependencies.

The indicator variable models were set up following procedures outlined in Kleinbaum and Kupper (1978). For k classes, $k-1$ indicator variables (z) are developed where $z_i = 1$ if class i is true, $z_i = 0$ if class i is not true, and all $z_i = 0$ for $i = 1, \dots, k-1$ when class k is true. In the simplest case with one independent variable (x) and one indicator variable (z) the model would take the form:

$$y = \beta_0 + \beta_1.x + \beta_2.z + \beta_3.xz + error$$

This general case can be expanded to include any number of independent and indicator variables. In the multiple-linear regression case a multiple-partial F test is used to determine whether the inclusion of the indicator variables produces a significant change in the error mean square (Kleinbaum and Kupper 1978). That is, one can test the null hypothesis that the effect of any given explanatory variable is independent of the indicator, or group effect.

It is standard to develop a full indicator variable

Table 1. Correlation coefficients between all independent variables. The terms are mean patch size (psz_i), mean interpatch distance ($pdst_i$), shannon index (H'), variance mean ratio (vmr_i), and initial proportion (P_{i0}).

	psz_i	$pdst_i$	H'	vmr_i	P_{i0}
psz_i	1.0	0.82	-0.09	0.55	0.11
$pdst_i$		1.0	-0.50	0.74	-0.38
H'			1.0	-0.69	0.90
vmr_i				1.0	-0.60
P_{i0}					1.0

model and test the stability of that model when the class effect is ignored for one or more of the explanatory variables. However, we have taken an alternative approach. Due to the large number of variables in the full indicator model (30) and the relatively small sample size (100) it was considered prudent to start with the linear model with no class effect, and add the class effect separately for each of the explanatory variables. The significance of the class effect was then established for each variable individually. This approach avoids the situation of comparing the error mean square of two overfit models. A forward stepwise regression was also used to identify the best model that includes the indicator variables.

Tree-based models were constructed as another approach to understand the influence of the explanatory variables on the scaling behavior. Regression tree analysis is a procedure for recursively splitting a dependent variable into increasingly homogeneous subsets based on a set of categorical or continuous explanatory variables. During each iteration, the best partitioning of the data is generated based on the explanatory variable which, upon splitting at some break point, will produce the greatest reduction in the error sum of squares. The break points are determined using a least squares criteria. A graphic representation of a tree-based model is structured so that one can follow the tree from the top node (*root*), through a series of binary decision rules on the explanatory variables (*branches*), to an end node (*leaf*) (Fig. 4). The mean of all observations which follow the same series of branchings from the root to a given leaf represents the estimated value of the dependent variable. Once

developed, trees can be *pruned* by removing splits which do not contribute greatly to the predictive power of the model. Tree-based models are well suited for situations where the set of predictors consists of both numeric variables and ordered factors and are useful for investigating nonlinear or non-systematic relationships. They also permit easy interpretation of the relationships between predictors and the response variable, and can expose interactions among the set of predictors. Tree-based models are described in Chambers and Hastie (1992).

Regression trees are typically overdeveloped and then pruned back to avoid overfitting the data. In this analysis, the size of the regression tree is determined following a simple cross-validation procedure employed by Davis *et al.* (1990). The dataset is iteratively divided into random subgroups each of which is used both to develop and test a model. As the tree grows, the cross-validated performance increases up to a critical tree size. Beyond this size, model performance falls off as additional branches are 'sprouted' in response to peculiarities in the development data but fail to account for any variance in the test data. The point at which this occurs indicates the appropriate number of terminal nodes to use in developing a tree from the entire dataset (Chambers and Hastie 1992; Davis *et al.* 1990).

Results and discussion

Multiple-linear regression model

Forward and backward stepwise procedures were used to determine the best number of variables to include in the standard model, and to identify which variables contributed consistently to explaining the variance in estimation error (E_{ir}). Examination of the change in the error sum of squares (SSE) with iterative addition (or subtraction) of variables, and examination of the order that the variables entered (or were removed) led to the selection of initial proportion (P_{i0}), variance/mean ratio (vmr_i), mean patch size (psz_i), mean interpatch distance ($pdst_i$) and resolution (r). Table 1 is a correlation matrix for the independent variables used. Note that while

Table 2. Regression summary for the best standard multiple-linear model. The variables are listed in the order that, at each step, results in the largest increase in adjusted R^2 . The R^2 values represent the new adjusted R^2 that results upon the addition of each variable.

	Coefficient	Standard error	t-value	P > t	Adjusted R-square
Intercept	-1.41	0.083	-13.6	0.000	NA
Initial proportion	3.14	0.218	14.4	0.000	0.15
Variance-mean ratio	0.07	0.006	11.8	0.000	0.55
Patch size	-0.15	0.002	-8.5	0.000	0.57
Interpatch distance	0.035	0.004	7.9	0.000	0.73
Resolution	-0.034	0.012	-2.9	0.005	0.75

H' and P_{i0} are highly correlated, H' is only used in the regression tree model and P_{i0} is only used in the linear model. Table 2 shows the summary statistics for the best linear model. The variables are listed in Table 2 in the order that, at each step, results in the largest increase in adjusted R^2 . The adjusted R^2 values represent the new adjusted R^2 that results upon the addition of each variable. The t values for the coefficients indicate that the contribution to the model of all variables is significant at the $P = 0.01$ level. The overall model has an adjusted R^2 of 0.75.

The slope coefficients allow interpretation of the influence of the independent variables on the scaling of cover-type proportions. The first variable, initial proportion (P_{i0}), has a positive slope indicating that the magnitude and direction of proportion error (E_{ir}) is positively correlated with the original size of the class. Examples with large initial proportions will tend to develop positive estimation errors as the scene is aggregated. Small initial proportions will lead to negative errors. Assuming a random spatial distribution of all classes with different proportions, this fundamental relationship would govern completely the growth or demise of individual cover types (Turner *et al.* 1989a). This relationship is modified, however, by the spatial characteristics of the individual cover types in the scene (Moody and Woodcock 1994; Turner *et al.* 1989a). While P_{i0} is the most important single variable, the adjusted R^2 value for initial proportion on estimation error is only 0.15 (Table 2). Our interest is in the role of the spatial pattern variables in accounting for the deviation from this simple relationship between P_{i0} and E_{ir} .

The variance/mean ratio (vmr_i) has a positive coefficient. This corresponds with our intuitive understanding of the scaling process since large values of vmr_i indicate clumped distributions. Highly clumped classes should persist through the aggregation procedure and 'consume' more dispersed classes. If classes appear as large homogeneous patches that are widely dispersed, then they should maintain their proportions as long as these patches are large relative to the observation scale. This effect may counteract the influence of initial proportion described above. An obvious example is the *water* class composed of lakes scattered sparsely across the landscape. This is a small class with a high degree of aggregation, and its proportions typically increase up to resolutions of 510 or 1020 meters. Conversely, a disaggregated class should diminish faster (or grow less dramatically) than its aggregated counterpart assuming equal initial proportions.

While it is expected that classes with large patch sizes will increase with aggregation, the mean patch size variable (psz_i) has a negative coefficient. Moreover, it is known that, for this dataset, classes with large patch sizes (*conifer* and *water*) do in fact develop positive estimation errors with aggregation. However, while classes with small patch sizes do diminish, classes with moderately large patch sizes (especially *conifer*) tend to increase much more dramatically than classes with extremely large patches (*water*). This is due to other factors, such as initial proportion, which are also influential in determining how the cover types scale and may weaken the influence of patch size. Correlations between patch size, initial proportion, interpatch dis-

Table 3. Model variables for each class type by region at 510 m resolution. Regions are symbolized by R1 through R4. The symbols next to each entry in the left hand column correspond to the location of these classes in the regression tree diagram (Figure 4).

Data Matrix for Selected Variables (510 m)					
Class & Region	$E_{i,r}$	psz_i	$pdst_i$	vmr_i	P_{i0}
	Barren.R1**	-0.38	5.19	2.28	11.9
R2***	-0.69	3.07	1.90	8.51	0.06
R3***	-0.76	2.72	1.98	7.00	0.05
R4***	-0.60	3.10	1.97	8.90	0.04
Brush.R1++	-0.32	6.47	0.79	6.74	0.22
R2++	-0.23	6.78	0.72	7.20	0.22
R3**	-0.34	5.05	0.82	6.78	0.18
R4**	-0.35	4.39	0.49	5.95	0.20
Hardwood.R1***	-0.75	2.54	2.81	5.76	0.05
R2**	-0.32	5.17	1.38	8.13	0.13
R3*	-0.10	8.07	1.12	7.99	0.21
R4++	+0.01	8.59	0.59	6.62	0.27
Conifer.R1++	+0.26	61.2	0.73	4.98	0.59
R2++	+0.28	34.5	0.68	5.41	0.52
R3+	+0.26	36.5	0.40	5.09	0.51
R4+	+0.24	22.0	0.48	6.09	0.45
Water.R1++	+0.12	143	55.1	22.91	0.02
R2+++	+0.71	5.73	18.3	15.0	0.001
R3+	+0.06	35.8	11.3	22.13	0.01
R4+	+0.13	32.6	6.87	20.97	0.02

tance and variance/mean ratio (Table 1) further suggest that the expected influence of patch size on estimation error may already be accounted for by the presence of the other variables in the model. When patch size is used as the only independent variable, its coefficient is +0.0042 (standard error = 0.0009) supporting the basic concept that as patch size increases estimation error moves in a positive direction.

Mean interpatch distance ($pdst_i$) also has a positive coefficient. This suggests a counterintuitive effect that widely dispersed classes become larger with aggregation. Normally one would assume that closely spaced classes would grow and widely spaced examples would be consumed as aggregation progressed. In this case the coefficient for interpatch distance is probably influenced by the *water* class which is extremely aggregated, has large patch sizes, but also has large interpatch distances. As noted above, *water* deviates from the expected behavior for a class with low initial proportions by

developing positive estimation errors at all levels of aggregation. When the model is run with water excluded, the coefficient for interpatch distance changes to -0.10 . This change to a negative coefficient indicates that, generally speaking, large interpatch distances do correspond to negative estimation errors, and vice versa.

The coefficient for resolution (r) is negative indicating that, on the balance, there is a stronger tendency for classes to diminish rather than increase as the scene is aggregated to progressively coarser scales. This is easily explained by the fact that *barren*, *brush* and *hardwood* all typically decrease with aggregation, whereas only *water* and *conifer* increase. It is notable that resolution contributes little to explaining the variance in the estimation error (Table 2). This is probably because the positive and negative influences of r on estimation error for different class types counteract each other. This provides an important rationale for incorporating indicator variables as discussed below.

Numerous interactions between the important explanatory variables speak to the inherent complexity involved in understanding the scaling processes. For example, the low initial proportions and high interpatch distances typical for *water* suggest that this class should diminish, but these influences are mitigated by the high variance/mean ratio (and large patch sizes) and *water* almost always increases with aggregation. While this is an extreme example, it illustrates that the behavior of any given class is a complex function of the spatial characteristics. There are, however, some basic behaviors that can be illuminated by examining the model performance for subsets of the data.

Logical yet inconsistent interactions among the model variables control the magnitude and direction of estimation error. Table 3 displays the complete set of data at 510 m resolution and allows several observations which relate to interactions between the independent variables. Within each class, almost all examples which have either positive or relatively small negative estimation errors are associated with either a relatively large mean patch size, a small mean interpatch distance, a large variance/mean ratio, a large initial proportion, or some com-

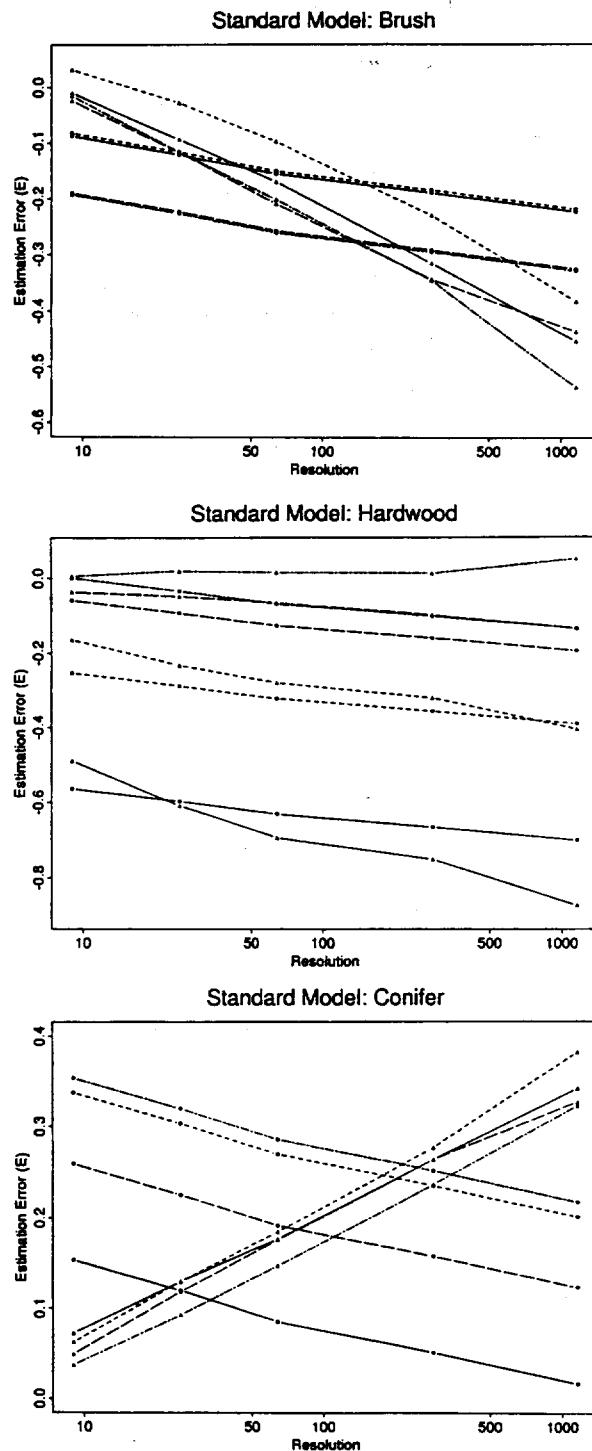


Fig. 2a-c. Comparisons of actual versus estimated E_{ir} values with resolution for the standard linear model. These are presented separately for (a) brush, (b) hardwood, and (c) conifer. The solid, short dashed, alternating dashed and long dashed lines represent regions 1, 2, 3 and 4, respectively. Solid triangles represent measured values and solid circles represent model estimates.

combination of the above. For example, *hardwood* in regions 3 and 4 have the smallest magnitude errors for this class and also have large patch sizes, low interpatch distances, moderate variance/mean ratios, and large initial proportions. All examples with large negative errors have the opposite associations. For example, *hardwood* in region 1 shows the largest magnitude error for this class and has the smallest patch size, largest interpatch distance, smallest variance/mean ratio and smallest initial proportion. Similar inferences, based on the relationships exposed by the overall model can explain nearly every measured estimation error. However, these inferences are not always dependent on the same combination of attributes.

The results suggest a fairly strong predictive ability of the standard model. However, by examining the model performance for subsets of the data, it becomes clear that the scaling effects cannot adequately be approximated by a single linear model of this nature. Figures 2a through 2c are plots of estimation error versus resolution for the individual class types *brush*, *hardwood* and *conifer*. Two patterns are apparent in Fig. 2. First, the model typically overestimates the magnitude of estimation error at fine resolutions and underestimates the magnitude at coarse resolutions. This results from the need for a single linear model to accommodate both examples that grow and those that decrease in size. As a result, the model performs well overall, but provides a poor fit for the individual classes. An exception to this is *hardwood* (Fig. 2b), for which the model appears well suited. Second, the model completely fails to explain the sign of the slope of estimation error with increasing aggregation for the *conifer* class (Fig. 2c). This occurs because the model is most heavily influenced by classes which diminish rather than grow as the scale is degraded. The inability of the model to respond to the different behavior of the individual classes provides motivation to investigate alternative approaches.

Indicator variable model

As described in the *Methods* section, the class-type effect was added to the original standard model separately for each variable. For example, to test

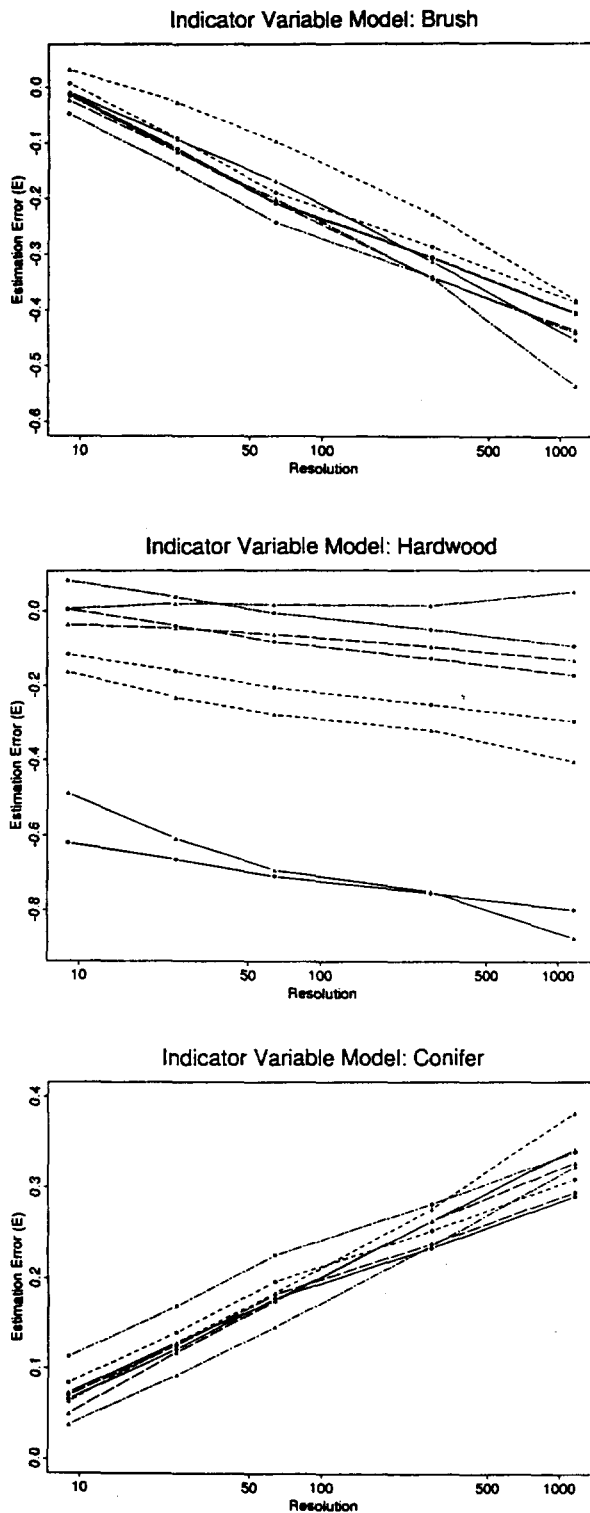


Fig. 3a-c. Comparisons of actual versus estimated E_r values with resolution for the best indicator variable model. Interpretation is the same as for Fig. 2.

whether the influence of initial proportion on estimation error differs between cover types when all other variables (vmr_i , psz_i , $pdst_i$ and r) are already included, the model with indicator variables (z_i):

$$E = \beta_0 + \beta_1 \cdot z_1 + \beta_2 \cdot z_2 + \beta_3 \cdot z_3 + \beta_4 \cdot z_4 + \beta_5 \cdot P_0 + \beta_6 \cdot vmr + \beta_7 \cdot psz + \beta_8 \cdot pdst + \beta_9 \cdot r + \beta_{10} \cdot P_0 \cdot z_1 + \beta_{11} \cdot P_0 \cdot z_2 + \beta_{12} \cdot P_0 \cdot z_3 + \beta_{13} \cdot P_0 \cdot z_4 + error$$

was compared to the standard model:

$$E = \beta_0 + \beta_1 \cdot P_0 + \beta_2 \cdot vmr + \beta_3 \cdot psz + \beta_4 \cdot pdst + \beta_5 \cdot r + error$$

using a multiple-partial F test. The F test indicates whether the two models are coincident. The equivalent test was performed for each of the original variables.

The F values are compared to a significant $F_{8,86,0.99}$ of 2.74. Based on this criteria, only resolution, with an F value of 23.54, produces a significant change in the model, indicating that the coefficient for resolution is not the same for all class types. This is not surprising as we have shown that different classes behave differently as a function of resolution (Fig. 3). Accounting for this class effect increases the adjusted R^2 from 0.75 to 0.91, and reduces the residual sum of squares from 2.60 to 0.814. Once the class-type interaction with resolution was in the model, factoring in the class effect on any of the remaining variables (P_{10} , vmr_i , psz_i , $pdst_i$) did not produce significant results when tested against a significant $F_{8,82,0.99}$. These results suggest that the effect of the spatial variables are relatively consistent across class types whether or not the class-type dependence of the resolution effect is accounted for. A few exceptions are discussed below.

A forward stepwise regression procedure was used to determine the best model that includes the indicator variables. Summary statistics for this model are presented in Table 4. Several observations can be made. First, there is a strong class-type effect on the resolution variable. Notice that the resolution coefficient for *conifer* and *water* (row 5 in Table 4) is positive, reflecting the general enlargement of these classes with aggregation. Conversely, the resolution coefficients for *barren*, *brush* and

Table 4. Regression summary for the best multiple linear model that includes indicator variables for class type. The indicator variables z_1 through z_4 represent *barren*, *brush*, *hardwood* and *water*, respectively. The character z_0 represents *conifer*. Note that the actual slope coefficient for the variance/mean ratio (*vmr*) for *water* is the sum of the two *vmr* coefficients ($-0.09 + 0.04$). Similarly for all other variables that have an individual class effect. Likewise, the intercepts for *barren* (z_1) is $-0.23 + -0.21$, the intercept for *water* (z_1) is $1.14 + -0.21$, and the intercept for *brush*, *hardwood* and *conifer* is simply -0.21 .

	Coefficient	Standard error	t-value	P > t
Intercept (z_2, z_3, z_0)	-0.21	0.065	-3.2	0.002
Intercept (z_1)	-0.23	0.065	-3.5	0.001
Intercept (z_4)	1.14	0.150	7.6	0.000
Variance-mean (z_1, z_2, z_3, z_0)	0.04	0.010	4.4	0.000
Resolution (z_4, z_0)	0.06	0.009	6.2	0.000
Variance-mean * z_4	-0.09	0.012	-7.5	0.000
Patch size * z_3	0.02	0.007	3.25	0.002
Interpatch distance * z_3	-0.24	0.022	-11.0	0.000
Resolution * z_1	-0.20	0.017	-11.3	0.000
Resolution * z_2	-0.15	0.009	-16.8	0.000
Resolution * z_3	-0.10	0.017	-5.9	0.000

hardwood (rows 9 through 11) are negative, reflecting the shrinkage of these classes. This achieves the separation of the data cases which grow and those which shrink as a function of resolution. Second, the coefficients for patch size (row 7 in Table 4) and interpatch distance (row 8) are positive and negative, respectively. The signs of these coefficients are as expected (unlike the standard linear model) but they are only important for the *hardwood* class. Third, the only important spatial variable for *all* class types is the variance/mean ratio. This is indicated in row 4, which accounts for the *vmr_i* effect on *barren*, *brush*, *hardwood* and *conifer*, as well as in row 6, which accounts for the *vmr_i* effect on *water*. The consistently significant effect of this variable suggests that the relative randomness, aggregation or disaggregation of the spatial distribution may be the most important spatial characteristic that modifies the general effect of initial proportion on scale-dependent proportion error. Finally, the initial proportion variable (P_{i0}) is conspicuously absent, the effect of which is probably already explained by the other variables in the model. The adjusted R^2 for this model is 0.92, and the residual sum of squares is 0.77.

The fact that resolution responds strongly to the indicator variables implies that there is an effect that is not accounted for by the other independent measures. This may be because region-wide values were used for psz_i , $pdst_i$, vmr_i and P_{i0} rather than

local values. That is, there may be so much variability across regions that it is difficult to provide general measures on a region-wide basis. It is also possible that there is some other effect which we are failing to account for in the model. This may relate to the resampling method.

Results from the indicator variable model summarized in Table 4 are presented in Figs. 3a through 3c. While the indicator variable approach adds substantial complexity to the model. Figure 3 shows considerable improvement in the estimated values of E_{ir} . Note in particular the improved estimates for *conifer* (Fig. 3c).

Regression tree model

The set of variables tested for the tree-based model include initial proportion (P_{i0}), variance/mean ratio (vmr_i), patch size (psz_i), interpatch distance ($pdst_i$), resolution (r) and the Shannon index (H'). The variables that contribute significantly to the reduction of the SSE for the model are psz_i , r , and H' . The number of terminal nodes was determined by the cross-validation procedure outlined in the *Methods* section. The goodness of fit criterion (residual sum of squares) was minimized at 12 terminal nodes when the model was applied to that portion of the data that was not used to develop it. The final tree was constrained to 12 nodes based on this criterion.

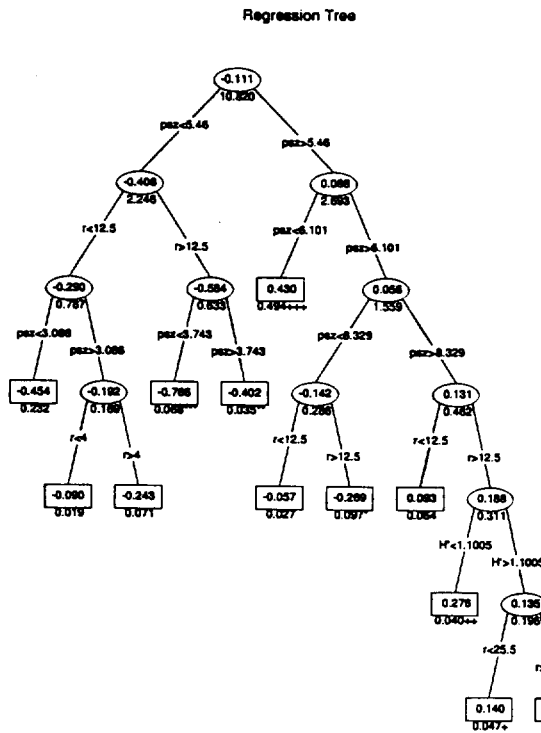


Fig. 4. Regression tree structure for the Plumas data. Ovals and squares represent non-terminal and terminal nodes, respectively. The values inside the ovals or squares are the estimates (or means) of all samples which flow through the tree to that particular node. The values beneath the estimates are the RMS-errors associated with using the mean as the estimate for all samples which flow through that node. Values along the internode connections are critical thresholds of given variables which provide the basis for the subsequent split and calculation of the estimates and RMS-errors. The symbols below the end nodes (*'s and +'s) correspond to the symbols next to the classes in Table 3 and represent the locations of the table entries on the tree diagram.

Figure 4 is a diagram of the regression tree for the Plumas data. The R^2 value for this model is 0.88. Of the two variables which carry any information about the spatial characteristics of the scene (psz_i and H') patch size dominates the discrimination structure, with H' only serving to guide one discrimination toward the extremity of the tree. Patch size is the single most important variable in the model. All samples with patch sizes below 5.46 have negative estimates of proportion error and almost all samples with values above this threshold have positive estimates. An interaction between patch size and resolution in determining the magnitude of the estimates is evidenced by the alternating splits

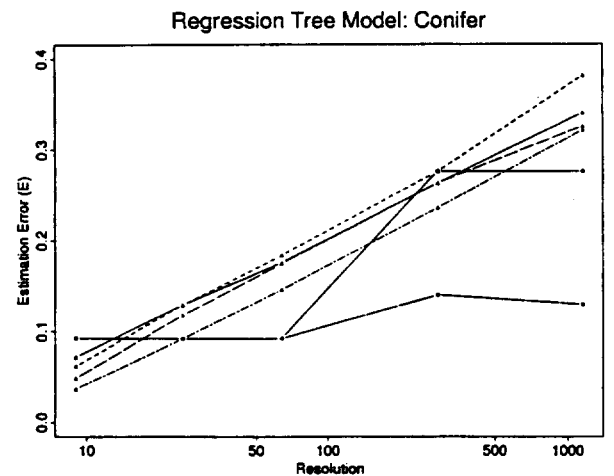
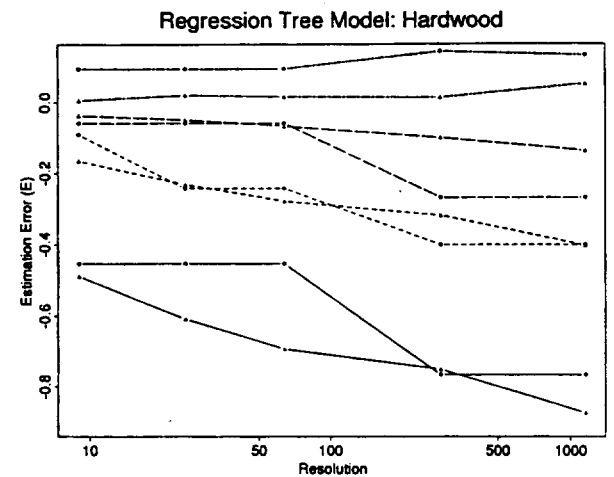
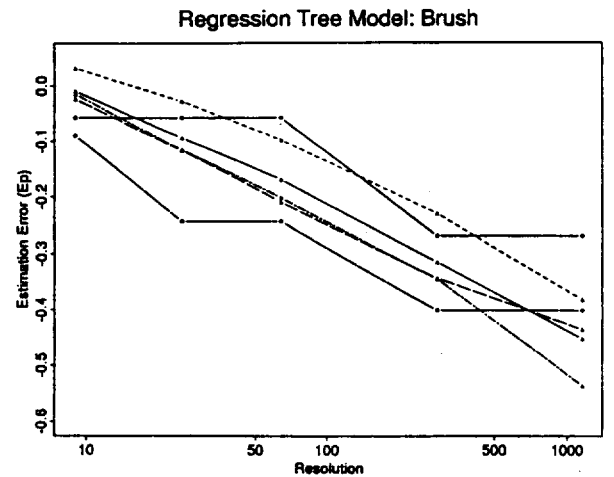


Fig. 5a-c. Comparisons of actual versus estimated E_{ir} values with resolution for the regression-tree model. Interpretation is the same as for Figs. 2 and 3.

on these two variables down the left side of the tree. There appear to be two critical scale transitions. The first and probably most important is between 240 m and 510 m (indicated by the threshold value of 12.5 in linear resolution units) which occurs near the top of the left portion of the tree and twice on the right side. The other is between 510 m and 1020 m (threshold value of 25.5) which appears toward the outer extremities.

Figures 5a through 5c are plots of estimation error versus resolution for the individual class types for the Plumas. A comparison of Fig. 5 with Fig. 2 shows that the tree-based model better follows the scale-dependent trends in estimation error than the standard linear model. Again, note the improved estimates for *conifer* (Fig. 5c). While the standard linear model cannot account for the shift in the slope direction of the relationship between estimation error and observation scale, the regression tree, like the indicator variable model does partition the data successfully into examples which grow in size and those which shrink as the scene is aggregated to coarser scales. Although the tree-based model is slightly weaker, it is considerably simpler than the indicator variable model. That is, the degree of growth or shrinkage is usually governed by some interaction between patch size and resolution. All but one of the end nodes in the tree are preceded by splits on critical thresholds based on these two variables. The strong performance of the regression tree may in part be due to overfitting. This problem occurs frequently with regression trees when applied to relatively small datasets. We attempted to avoid this problem by using the cross-validation procedure outlined in the *Methods* section.

Implications for coarse-scale mapping

Efforts to map global land cover should incorporate an understanding of how the definition and mapping of land-cover classes at coarse scales relate to the heterogeneity of the surface. This relationship is important not only for assessing the reliability of land-cover maps, but also to provide error information that may aid potential users in ap-

plying the data for their specific purposes. We present some approaches for relating the spatial characteristics of land-cover classes to the scaling of cover-type proportion estimates and the results have several implications along these lines.

In this work we have used a simple grid-based aggregation procedure that imposes an artificial spatial structure on top of the actual spatial distributions in the scene. This is partially analogous to the remote sensing situation. Understanding the interaction between landscape spatial characteristics and sampling resolution may allow improved methods for scaling high resolution land-cover data to coarser resolutions. This is particularly important for the validation and evaluation of coarse-scale land-cover classification results from remotely sensed data. It may also be possible to develop methods for correcting coarse resolution land-cover proportion measurements to estimates of actual proportions based on scaling models which are calibrated on region specific test sites. Several such methods are being assessed currently, but these depend on the intraregional stability of the scaling relationships.

Only one site is considered in this analysis and no external validation of the models is attempted at this stage. While the basic structures of these models should have some level of extensibility, it is expected that fundamentally different landscapes will scale in distinctive ways. Alternative measures of spatial pattern, or different thresholds and coefficients will be more useful in accounting for the scaling properties in different landscape types. The extensibility of these relationships should be assessed over a variety of landscapes and should incorporate additional spatial measures at a wide range of scales using many subregions.

A large array of spatial measures could have been used in this analysis, but we chose several on the basis of past research and in the interest of simplicity. These may not be the *best* measures, however, and the development and understanding of measures of spatial structure is an important avenue of research. Spatial measures such as fractal dimension, semi-variance, cross-correlation, Moran's I, or other measures of spatial non-randomness are widely cited and warrant investigation in this con-

text (Cullinan and Thomas 1992; Cressie 1993; Li and Reynolds 1993; Marceau *et al.* 1994). Moreover, an understanding of the scale-dependence of spatial pattern itself, such as presented in Turner *et al.* (1989a), might allow a better formulation of efforts to model scale-dependent proportion error. It is possible that a taxonomy of general scaling functions can eventually be developed which will allow the implementation of separate models depending on the type of landscape under consideration.

Conclusions

Previous research demonstrated that large proportion errors arise as land-cover data are sampled at progressively coarser scales (Moody and Woodcock 1994). Such errors have significant implications for coarse-scale modeling and monitoring activities that rely on land-cover datasets derived from remote sensing. An understanding of the role of spatial characteristics in governing the loss of information with decreasing resolution may improve our ability to preserve this information across scales or to quantify the errors expected in coarse-scale surface representations. Our results indicate significant relationships between the spatial characteristics of cover types and scale-dependent proportion errors. A related trend was found earlier by Turner *et al.* (1989a).

Generally speaking, as patch size, variance/mean ratio, and initial proportions of cover types increase, the proportion errors for those cover types move in a positive direction as the data are aggregated. Similarly, as these measures decrease, the tendency of a cover type to withstand aggregation and maintain its initial proportion decreases. The opposite relationship tends to hold for interpatch distance (when *water* is ignored) with greater distances leading to a disappearance with aggregation and vice versa. In the linear models there is strong interaction among the variables.

While the standard linear model performs fairly well for the dataset as a whole, it is unable to predict the fundamentally different behavior between samples which have positive and negative estimation

errors. Moreover, the sign and magnitude of the slope coefficients in the standard linear model, may be largely influenced by the need for this type of model to accommodate samples that scale in distinctly different ways. By allowing the slope coefficients of the independent variables to vary as a function of cover type, a significant improvement in the model is achieved. Several notable observations emerged. First, the significant interaction between class type and resolution implies that there is some important landscape property that is not accounted for in the model. Second, the lack of interaction between class type and the spatial variables indicates that these variables have relatively consistent influence across cover types. Third, the degree of nonrandomness (as measured by the variance/mean ratio) appears to be the most influential variable in modifying the interactive influence of initial proportion and scale on estimation error.

The regression tree model captures the scaling of proportion error primarily on the basis of interactions between patch size and aggregation scale. A threshold in patch size acts to split the dataset into a set of samples with negative errors and a set with positive errors. Interactions between patch size and two critical thresholds in resolution then partition the data into different levels of positive and negative errors. This model is successful at fitting the scaling process and is less complex in terms of the number of variables in the model and the interactions among variables.

We present an analysis of the relationship between land-cover spatial patterns and the scaling of cover-type proportions. The primary concern is the role of fine-scale landscape pattern in influencing the relationship between the scale of representation and cover-type proportion error. Results from both the linear regression and the regression tree models suggest that the interactive effects of spatial patterns and observation scale on proportion error can be understood and modeled using fairly simple measures of landscape spatial characteristics. It is hoped that relationships based on simple measures such as those presented here will lead to some generalizable understanding of scaling processes for a variety of landscape types.

Acknowledgements

This work was supported by the National Aeronautics and Space Administration under contract NAS5-31369. The authors gratefully acknowledge John Collins, Vida Jakabhazy, Scott Macomber and Soren Ryherd for their work in producing the Plumas land cover classification. Thanks also go to Alan Strahler for providing comments on an early draft of the manuscript, and to helpful comments from anonymous reviewers.

References

- Baker, W.L. and Cai, Y. 1992. The rule programs for multiscale analysis of landscape structure using the GRASS geographical information system. *Landsc. Ecol.* 7(4): 291–302.
- Baker, W.L. 1993. Spatially heterogeneous multi-scale response of landscapes to fire suppression. *Oikos* 66: 66–71.
- Chambers, J.M. and Hastie, T.J. 1992. *Statistical Models in S*. Wadsworth & Brooks/Cole Advanced Books and Software, Pacific Grove, CA.
- Cressie, N.A.C. 1993. *Statistics for Spatial Data*. John Wiley, New York.
- Cullinan, V.I. and Thomas, J.M. 1992. A comparison of quantitative methods for examining landscape pattern and scale. *Landsc. Ecol.* 7(3): 211–227.
- Davis, F.W., Michaelson, J., Dubayah, R. and Dozier, J. 1990. Optimal terrain stratification for integrating ground data from FIFE. *Proceedings of the American Meteorological Society, Symposium on FIFE*, Boston, MA, pp. 11–15.
- Field, C.B. and Ehleringer, J.R. 1993. Introduction: Questions of scale. In *Scaling Physiological Processes: Leaf to Globe*, pp. 1–4. Edited by J.B. Ehleringer and C.B. Field. Academic Press, San Diego.
- Gervin, J., Kerber, A., Witt, R., Lu, Y. and Sekhon, R. 1985. Comparison of level I land cover classification accuracy for MSS and AVHRR data. *Int. J. Remote Sens.* 6(1): 47–57.
- Getis, A. and Boots, B. 1978. *Models of Spatial Processes: An Approach to the Study of Point, Line and Area Patterns*. Cambridge University Press, Cambridge.
- Gopal, S. and Woodcock, C.E. 1994. Theory and methods for accuracy assessment of thematic maps using fuzzy sets. *Photogramm. Eng. Remote Sens.* 60(2): 181–188.
- Hess, G. 1994. Pattern and error in landscape ecology: A commentary. *Landsc. Ecol.* 9(1): 3–5.
- Jupp, D.L.B., Strahler, A.H. and Woodcock, C.E. 1988. Auto-correlation and regularization in digital images. *IEEE Trans. Geosci. Remote Sensing* 26(4): 463–473.
- Kleinbaum, D. and Kupper, L. 1978. *Applied Regression Analysis and Other Multivariable Methods*. Duxbury Press, Boston.
- Latty, R.S. and Hoffer, R.M. 1981. Computer-based classification due to the spatial resolution using per-point versus per-field classification techniques. *Machine Processing of Remotely Sensed Data Symposium*, West Lafayette, IN, pp. 384–392.
- Li, H. and Reynolds, J.F. 1993. A new contagion index to quantify spatial patterns of landscapes. *Landsc. Ecol.* 8(3): 155–162.
- Marceau, D., Howarth, P. and Gratton, D. 1994. Remote sensing and the measurement of geographical entities in a forested environment. 1. The scale and spatial aggregation problem. *Remote Sens. Environ.* 49: 93–104.
- Meentemeyer, V. and Box, E. 1987. Scale effects in landscape studies. In *Landscape Heterogeneity and Disturbance*, pp. 15–34. Edited by M. Turner. Springer-Verlag, New York.
- Milne, B. 1992. Spatial aggregation and neutral models in fractal landscapes. *Amer. Natur.* 139(1): 32–57.
- Moody, A. and Woodcock, C.E. 1994. Scale-dependent errors in the estimation of land-cover proportions – Implications for global land-cover datasets. *Photogramm. Eng. Remote Sens.* 60(5): 585–594.
- Nellis, M. and Briggs, J. 1989. The effect of spatial scale on Konza landscape classification using textural analysis. *Landsc. Ecol.* 2(2): 93–100.
- O'Neill, R., Krummel, J., Gardner, R., Sugihara, G., Jackson, B., Angelis, D., Milne, B., Turner, M., Zygmunt, B., Christensen, S., Dale, V. and Graham, R. 1988. Indices of landscape pattern. *Landsc. Ecol.* 1: 153–162.
- Raffy, M. 1992. Change of scale in models of remote sensing: A general method for spatialization of models. *Remote Sens. Environ.* 40: 101–112.
- Running, S., Justice, C., Hall, D., Huete, A., Kaufman, Y., Muller, J., Strahler, A., Vanderbilt, V., Wan, Z., Teillet, P. and Carneggie, D. 1994. Terrestrial remote sensing science and algorithms planned for EOS/MODIS. *Int. J. Remote Sens.* (in press).
- Salomonson, V., Barnes, W.L., Maymon, P.W., Montgomery, H.E. and Ostrow, H. 1989. MODIS: Advanced facility instrument for studies of the Earth system. *IEEE Trans. Geosci. Remote Sensing* 27: 145–153.
- Stoms, D. 1994. Scale dependence of species richness maps. *Prof. Geogr.* 46(3): 346–358.
- Strahler, A., Moody, A., Lambin, E., Huete, A., Justice, C., Muller, J., Running, S., Salomonson, V., Vanderbilt, V. and Wan, Z. 1994. *MODIS Land Cover Product Algorithm Technical Basis Document*. NASA document for MODIS Product No. 11, Parameter Nos. 2669 and 2671 (in review).
- Townshend, J. and Justice, C. 1988. Selecting the spatial resolution of satellite sensors required for global monitoring of land transformations. *Int. J. Remote Sens.* 9(2): 187–236.
- Townshend, J. and Justice, C. 1990. The spatial variation of vegetation changes at very coarse scales. *Int. J. Remote Sens.* 11(1): 149–157.
- Townshend, J.R.G. (Ed.) 1992. Improved global data for land applications: A proposal for a new high resolution data set. In *IGBP Global Change Report No. 20*, 87 pp. International Geosphere-Biosphere Program, Stockholm.
- Turner, M., O'Neill, R., Gardner, R. and Milne, B. 1989a.

- Effects of changing spatial scale on the analysis of landscape pattern. *Landscape Ecol.* 3(3/4): 153-162.
- Turner, M., Dale, V. and Gardner, R. 1989b. Predicting across scales: Theory development and testing. *Landscape Ecol.* 3(3/4): 245-252.
- Turner, S., O'Neill, R., Conley, W., Conley, M. and Humphries, H. 1991. Pattern and scale: Statistics for landscape ecology. In *Quantitative Methods in Landscape Ecology: The Analysis and Interpretation of Landscape Heterogeneity*, pp. 17-49. Edited by M. Turner and R. Gardner. Springer-Verlag, New York.
- Unwin, D. 1981. *Introductory Spatial Analysis*. New York: Methuen.
- USA-CERL. 1991. GRASS 4.0 User's Reference Manual. United States Army Corps of Engineers Construction and Engineering Research Laboratory, Champaign, Ill.
- Woodcock, C.E. and Strahler, A.H. 1987. The factor of scale in remote sensing. *Remote Sens. Environ.* 21: 311-332.
- Woodcock, C.E. and Gopal, S. 1992. Accuracy assessment of the Stanislaus Forest vegetation map using fuzzy sets. *Proceedings of the Fourth Biennial Remote Sensing Applications Conference*, Orlando, FL, April, 1992, pp. 378-394.
- Woodcock, C.E., Gopal, S., Macomber, S.A. and Jakabhazy, V.D. 1994. *Accuracy Assessment of the Vegetation Map of the Plumas National Forest*. Technical Report, Center for Remote Sensing, Boston University, 19 pp.
- Woodcock, C.E., Collins, J., Gopal, S., Jakabhazy, V., Li, X., Macomber, S., Ryherd, S., Wu, Y., Harward, V.J., Levithan, J. and Warbington, R. 1993. Mapping forest vegetation using Landsat TM imagery and a canopy reflectance model. *Remote Sens. Environ.* 50: 240-254.